

## CARBON IN PLANETARY NEBULAE

JAMES B. KALER

Department of Astronomy, University of Illinois  
 Received 1981 February 6; accepted 1981 March 26

### ABSTRACT

Carbon abundances, and in particular C/O ratios, are calculated for 53 planetary nebulae from the strength of the optical  $\lambda 4267$  C II line. Where necessary, the intensity of  $\lambda 4267$  is corrected for systematic error for each nebula by comparing it to nearly observed  $\lambda 4541$  He II,  $\lambda 4363$  [O III], and  $\lambda 4471$  He I lines whose true intensities are known from measurements of  $\lambda 4686$  He II,  $\lambda 5007$  [O III], or from accurate photometry of  $\lambda 4471$ . Total C/O ratios are derived on an arbitrary scale and then scaled to the C/O ratios that have been measured for eight nebulae from analyses of their far-ultraviolet spectra. The calculations assume that C II  $\lambda 4267$  is strictly a recombination line, and that  $C^{2+}/C$  follows an ionization curve which is the mean of the  $He^+/He$ ,  $Ar^{2+}/Ar$ , and  $Cl^{2+}/Cl$  curves. An empirical correction to allow for the effect of electron density on ionization is also made. Although some individual nebulae may have an excess of carbon, the median of the distribution of C/O values is similar to the solar value; this comparison, however, depends strictly upon the selection of and the scaling to the ultraviolet data. More significant are the relative C/O ratios herein derived, which do not support Becker and Iben's theoretical prediction that C/O becomes greatly enhanced as He/H increases. Perhaps a significant amount of carbon is tied up in molecules and grains. Other possibilities, and problems involving ionization and selection effects, are discussed.

*Subject headings:* nebulae: abundances — nebulae: planetary

### I. INTRODUCTION

This paper is the sixth and last in a current series which analyze the chemical compositions of planetary nebulae for the primary purpose of providing data for, and for the examination of, theories of stellar and galactic evolution. The previous five papers discuss (1) neon, argon, and chlorine; (2) helium; (3) nitrogen; (4) oxygen; and (5) sulfur: see Kaler (1978*a*, 1978*b*, 1979, 1980, 1981), respectively. The current paper completes the series with a discussion of carbon abundances, which are of critical importance in evaluating theory.

The subject of carbon abundances in planetary nebulae has produced an interesting controversy. The question of whether or not carbon is overabundant, or enriched, in these objects is not yet settled. Attempts at measurement of C/H ratios go back to Aller and Menzel (1945) who used the  $\lambda 4267$  C II recombination line and found high values of C/O. Much later, Torres-Peimbert and Peimbert (1977, hereafter TPP) used this line and  $\lambda 4650$  C III to come to a similar conclusion: that carbon is severely overabundant in planetaries.

It is now possible to observe the carbon lines in the ultraviolet, which should result in a more accurate evaluation of the abundances (Bohlin, Marioni, and Stecher 1975; Bohlin, Harrington, and Stecher 1978; Pottasch, Wesselius and van Duinen 1978; Harrington *et al.* 1980; Torres-Peimbert, Peimbert and Daltabuit 1980; Perinotto, Panagia, and Benvenuti 1980; Aller and Keyes 1981; Harrington *et al.* 1981; Lutz 1981). Some of this work indicates C/H close to solar, but the most recent authors still suggest enhanced C/H or C/O. Broadly, the ultra-

violet work shows lower carbon abundances than does the optical, but there is still a strong feeling for enrichment.

Becker and Iben (1980, hereafter BI) indeed predict that carbon should be overabundant in planetaries. They expect carbon to be brought to the surface of the star during the thermal pulsation stage that takes place on the asymptotic giant branch. They also predict a strong positive correlation between C/O and He/H. Unfortunately, there are currently only a limited number of nebulae that have been observed in the ultraviolet. In order to check the theory, a large number of nebulae should be used, which cover a broad range in He/H. It is the purpose of this paper to present a new method by which the widely observed  $\lambda 4267$  C II line can be used to derive C/O ratios as a first extensive check of the theory, and as a guide to individuals observing the carbon lines in the ultraviolet. Alternatively, after a large number of nebulae have been so observed, the data provided here will be of use in evaluating the theory of the production of the optical carbon lines. The  $\lambda 4650$  C III lines are not used because of a serious problem of blends with O II and because of the lack of an appropriate ionization curve (see below).

### II. CALCULATIONS OF CARBON ABUNDANCES

The calculation procedure produces carbon abundances after a series of five steps, outlined as follows:

a) correction of the  $\lambda 4267$  C II line intensity for systematic error when necessary;

b) computation of  $C^{2+}/H^+$  under the assumption that  $\lambda 4267$  C II is strictly a recombination line;

c) calculation of  $C^{2+}/O$ , and a total relative C/O ratio, by comparing  $C^{2+}/O$  with a value expected from the ionization level of the nebula.

d) empirical correction of the above for the effect of electron density on ionization level;

e) scaling of these results to C/H or C/O derived from current ultraviolet data.

#### a) Intensities of $\lambda 4267$ C II

The  $\lambda 4267$  C II line is always very weak, at most only a few percent of the  $H\beta$  intensity, and often well under one percent. Consequently, its measurement can be subject to systematic error, especially when it is at the lower intensity limit of a study that used photographic photometry. We now have available a sizable body of accurate photoelectric digital-scanner photometry (see especially Aller and Czyzak 1979). In order to produce a maximum-size sample of objects, however, the older data must be included. Fortunately, it is possible to evaluate the systematic error present in these data; there are other fairly weak lines in the wavelength neighborhood of  $\lambda 4267$  that were measured by the same reduction procedure as was  $\lambda 4267$ , and whose true intensities can be independently determined. A correction factor derived for these lines can then be applied to the intensity of the carbon line. Three lines,  $\lambda 4471$  He I,  $\lambda 4541$  He II, and  $\lambda 4363$  [O III], are suitable.

For high-excitation nebulae we can determine the true  $\lambda 4541$  intensity from Brocklehurst's (1971)  $I(\lambda 4541)/I(\lambda 4686)$  ratio, and the intensity of  $\lambda 4686$  that was measured by the same authors who observed  $\lambda 4267$ . In cases where  $\lambda 4541$  is observed,  $\lambda 4686$  is strong and generally accurately measured. Also for these nebulae we can calculate the true  $\lambda 4471$  intensity from the  $\lambda 4686$  intensity, which gives  $He^{2+}/H^+$ , and the known He/H ratio (Kaler 1978*b*, 1980). An accurately measured  $\lambda 4471$  intensity from another source cannot be used directly for the higher excitation objects because stratification may render that particular value inappropriate to the region of the nebula in which  $\lambda 4267$  was observed. For the low-excitation nebulae, however, a photoelectrically determined  $\lambda 4471$  intensity will suffice. The  $\lambda 4363$  [O III] line can be used when the helium lines are not available, or as a check. We know the  $I(\lambda 5007)/I(\lambda 4363)$  ratio from photoelectric photometry, where we assume that the electron temperature of the nebula is constant. Usually, however,  $\lambda 4363$  is too strong to provide a meaningful correction. The final correction factor is the mean of those available, where the  $\lambda 4541$  correction has the most weight because it is subject to the fewest errors. The corrections are nearly all in the sense that  $I(\lambda 4267)$  is overestimated. The factors average about 0.7, and range from about 0.3 to 1. The error in this factor, as derived from high excitation nebulae where two values are available, averages about  $\pm 20\%$ , but it may be much higher for specific nebulae. Intensities from recent scanner work are assumed to be free of systematic error.

Table 1 presents the catalog of intensities, where columns (1) and (2) give the nebula's common name and the Perek-Kohoutek (1967) number, respectively. Columns (3) and (4) give the intensities of  $\lambda 4267$  on the scale  $I(H\beta) = 100$ , corrected for interstellar extinction. The Aller and Czyzak (1979) data (plus those for two nebulae not in their list) are presented in column (3); column (4) contains all other data, to which correction has been applied where necessary. The references for the intensities in column (4) are given in column (5), and the region in which the line was observed in column (6). The code names conform to those used in Kaler's (1976) catalog, where data on extinction constants can be found. See the more recent references themselves (AC79, AKRO, AROK, TPP, TPP2, and KON) for extinction information.

A subjective relative weight from 1 to 4 is assigned to each of the column (4) intensities in column (7), where weight 4 indicates the probability of the lowest error. The weights are assigned on the basis of how the observed  $\lambda 4267$  intensity compares with the three weakest lines observed in that wavelength neighborhood by the authors listed in column (4). The weighting criteria for the corrected intensities are as follows:

1:  $I(\lambda 4267)$  among the weakest lines;

2:  $I(\lambda 4267)$  the order of 1.5 times stronger than the weakest lines;

3:  $I(\lambda 4267)$  between 2 and 5 times stronger;

4:  $I(\lambda 4267)$  more than 5 times stronger.

If the correction factor is less than  $\sim 0.6$ , the weight is reduced by one. The recent scanner work, including the AC79 values in column (3), are generally given weight 4.

The intensities in Table 1 are the most complete and accurate set available. The true errors of the column (4) data, however, are largely not known; the weights provide only a measure of relative error. The correction factor really applies to  $\lambda 4541$  and  $\lambda 4471$  which can be anywhere from 2 to 10 times the strength of  $\lambda 4267$ . The

---

REFERENCE KEY TO TABLE 1.—AC70: Aller and Czyzak (1970). AC79: Aller and Czyzak (1979). ACPG: Aller and Czyzak (unpublished photographic measurements). AE: Aller and Epps (1975). AK1: Aller and Kaler (1964*a*). AK2: Aller and Kaler (1964*b*). AK3: Aller and Kaler (1964*c*). AKB: Aller, Kaler, and Bowen (1966). AKI: Aller, Kaler, and Czyzak (1976). AKRC: Aller, Krupp, and Czyzak (1969). AKRO: Aller, Keyes, Ross, and O'Mara (1981). AKY: Aller and Keyes (1981).<sup>f</sup> AROK: Aller, Ross, O'Mara, and Keyes (1981). AW: Aller and Walker (1965). AWR: Aller and Wares (1969). BHS: Bohlin, Harrington and Stecher (1978).<sup>f</sup> BMS: Bohlin, Marionni, and Stecher (1975).<sup>f</sup> CA70: Czyzak and Aller (1970). CA73: Czyzak and Aller (1973). CAK1: Aller, Czyzak, and Kaler (1968). CAK2: Czyzak, Aller, and Kaler (1968). CAK4: Czyzak, Aller, and Kaler (1971). CAKF: Czyzak, Aller, Kaler, and Faulkner (1966). CAL: Czyzak, Aller, and Leckrone (1969). HLS: Harrington, Lutz, and Seaton (1980).<sup>f</sup> quoted in HLSS. HLSS: Harrington, Lutz, Seaton, and Stickland (1980).<sup>f</sup> LU4: Lutz (1981).<sup>f</sup> KACE: Kaler, Aller, Czyzak, and Epps (1976). KCA: Kaler, Czyzak, and Aller (1968). KON: Kondratyeva (1978). LAKC: Lee, Aller, Kaler, and Czyzak (1974). PPB: Perinotto, Panagia, and Benvenuti (1980).<sup>f</sup> PWD: Pottasch, Wesselius, and van Duinen (1978).<sup>f</sup> TPD: Torres-Peimbert, Peimbert, and Daltabuit (1980).<sup>f</sup> TPP: Torres-Peimbert and Peimbert (1977). TPP2: Torres-Peimbert and Peimbert (1979).

<sup>f</sup> Source of ultraviolet data.

TABLE 1  
 $\lambda 4267$  C II INTENSITIES, AND C/O, C/H RATIOS

Nebula (1)	PK (2)	I(H $\beta$ )=100		Ref. (5)	Reg. (6)	wt. of col.(4) (7)	(C/O) <sub>1</sub> (8)	(C/O) <sub>2</sub> (9)	10 <sup>4</sup> (C/H) <sub>2</sub> (10)	wt <sub>2</sub> (11)	UV Ref (12)
		AC79 $\lambda\lambda 4267$ (3)	Other $\lambda\lambda 4267$ (4)								
NGC 650	130-10°1	0.79					0.57	0.26	2.1	2	
1535	206-40°1	1.02	0.49	ACPG		2	1.8	1.2	3.5	4	
2022 <sup>a</sup>	196-10°1	0.89	1.43	AC70		3	7.3	2.7	14	3	
2371 <sup>b</sup>	189+19°1		0.37	AGPG	R	1	1.9	0.76	2.7	1	PWD
2371	189+19°1		0.47	ACPE	F1	1		--	--	--	
2440 <sup>b</sup>	234+ 2°1	0.40 <sup>c</sup>	0.40	CAK1		4	0.86	0.35	1.6	4	AKY
2867	278- 5°1		0.90	AKRO		4	0.97	0.49	2.8	3	
3242 <sup>b</sup>	261+32°1	0.72	0.73	CAKF		4	1.04	0.83	3.5	4	PWD
6210	294+43°1		0.40	ACB		3	0.37	0.36	1.6	3	
6302	349+ 1°1		0.15	AROK		4	0.29	0.49	1.0	3	
6309 <sup>a</sup>	9+14°1		0.57	CA70	C1+C2	1	1.3	0.84	4.2	1	
6543 <sup>b</sup>	96+29°1	0.66	1.02	CAK2		4	0.65	0.45	2.4	4	PWD
6572	34+11°1	0.40	0.72	AK2		4	0.77	0.87	2.8	4	
6644	8- 7°2		0.43	AKI		1	0.69	0.60	2.1	1	
6720	63+13°1		0.94	AW		1	1.5	0.41	1.7	1	
6741	33- 2°1		0.69	AKRC		2	0.77	0.45	2.8	2	
6778	34- 6°1	2.51	3.37	CA73	CR+PG	4	8.0	4.2	7.1	3	
6790	37- 6°1	0.31					0.43	0.52	2.0	3	
6803	46- 4°1		0.47	LAKC		2	0.49	0.50	2.2	2	
6804 <sup>a</sup>	45- 4°1		1.12	ACPG		1	>3.9	>1.3	>5	1	
6818 <sup>a</sup>	25-17°1	0.44					0.91	0.53	3.3	4	
6826	83+12°1		0.73	CAKY		3	0.95	0.47	1.5	3	
6833	82+11°1		0.22	AKI		1	0.75	0.78	0.92	1	
6884	82+ 7°1	0.47	0.72	AKI		2	0.57	0.58	2.7	4	
6886	60- 7°2	0.44					0.71	0.57	2.9	4	
6891	54-12°1		0.91	AKI		2	1.3	0.73	2.0	2	
7008 <sup>a</sup>	93+ 5°2		3.2	ACPG		2	11	11	60	1	
7009	37-34°1	0.67 <sup>d</sup>	0.88	AKI+AE	CB	4	1.1	0.55	2.0	4	
7026	89+ 0°1	0.78	0.95	CA70	FM+IR	3	0.85	0.10	0.55	3	
7027 <sup>b</sup>	84- 3°1		0.68	KACE		4	0.88	1.7	9.9	4	PWD BMS FPB
7662 <sup>a,b</sup>	106-17°1	0.62	0.57	AKB		3	1.8	1.2	3.9	4	PWD BMS HLS
IC 351	159-15°1	0.45	0.95	AW		1	1.2	0.84	3.3	4	
IC 418	215-24°1	1.48	0.73 0.46	AK3 TPD		4	1.0	1.8	16	3	TPD HLSS
1747	130+ 1°1	0.68	1.34	CA70		2	0.59	0.37	2.0	4	
2003	161-14°1	0.44	0.84	AC70		2	0.75	0.49	2.1	4	
2149	166+10°1		0.73	TPP		3	2.4	1.3	2.7	2	
2165	221-12°1	0.41	0.32	KCA		3	1.1	0.63	2.0	4	
4642 <sup>a</sup>	334- 9°1		1.28	AWR		1	12	2.9	12	1	
4997 <sup>e</sup>	58-10°1		0.19	AK2		4	--	--	--	--	
5117	89- 5°1	0.43					0.37	1.0	5.5	2	
5217	100- 5°1	0.22	0.26	CAL		1	0.32	0.31	1.1	4	
Cn 3-1	38+12°1	0.30					4.9	3.4	8.1	3	
Ha 4-1	49+88°1		1.38	TPP2		3	2.9	0.84	1.8	3	
Hu 1-2 <sup>a</sup>	86- 8°1	0.32	0.17	AW		1	1.8	1.8	3.5	3	
Hu 2-1 <sup>b</sup>	51+ 9°1	0.36					.58	0.65	2.4	3	LU4
J 320	190-17°1	0.40					.93	0.51	0.92	3	
J 900	194+ 2°1	0.83					1.9	1.5	5.4	3	
M1-5	184- 2°1		1.98	KON		1	4.3	3.1	8.5	1	
M1-14	235- 1°1		4.3	KON		2	13	16	36	1	
M1-74	52- 4°1	0.54					0.53	0.45	2.1	3	
M1-80	107- 2°1		1.6	KON		1	3.3	1.9	7.5	1	
M2-50	97- 2°1		1.9	KON		1	3.5			1	
Vy 1-1	118- 8°1		0.15	KON		1	0.37	0.29	0.65	1	
Vy 1-2	53-24°1		0.30	KON		1	0.24	0.21	1.7	1	

<sup>a</sup> He<sup>2+</sup>/He<sup>+</sup> > 1, O/H may be unreliable for these nebulae. 10<sup>4</sup> O/H follows in parentheses: NGC 2022 (5.05); NGC 2371 (4.47); NGC 6309 (4.97); NGC 7008 (5.1); IC 4642 (4); Hu 1-2 (1.24); He/H not known for NGC 6804.

<sup>b</sup> Used for scaling to UV data.

<sup>c</sup> Aller, Keyes, Czyzak, and Shields (1981).

<sup>d</sup> Czyzak and Aller (1979).

<sup>e</sup> No values of (C/O) + (C/H) computed because of high and uncertain density.

results in Table 1 assume that the error for the weak lines is independent of intensity, which may not be correct.

b) *Initial Calculation of  $C^{2+}/H$*

We may perform this second step by using the equation

$$\frac{C^{2+}}{H^+} = 1.09 \times 10^{-3} t^{0.14} I(\lambda 4267), \quad (1)$$

where  $t = T_e \times 10^{-4}$ , which was derived by TPP using Pengelly's (1963) and Brocklehurst's (1971) effective recombination coefficients for C II and H. It is assumed that  $\lambda 4267$  is caused by recombination only and that there is no fluorescent contribution, for which there is generally good evidence; see TPP and Grandi (1976) for a discussion of this problem.

Two intensities are given for NGC 2371; regions *B* and *E1* are respectively of high and low excitation. Only the former is used in the abundance calculations since it requires a much smaller correction factor, it is more representative of the nebula as a whole, and a better electron density is available.

c) *The Ionization Curve*

The third step involves the process of correcting for unobserved ions, generally  $C^+$  and  $C^{3+}$ ; that is, we must go from the ionic abundance of  $C^{2+}$  to the total abundance of carbon. The procedure used is a modification of the one developed by Seaton (1968) and Peimbert and Costero (1969), who assess the contributions of unobserved ions by the known ionic abundance ratios of other elements with similar ionization potentials. If  $C/O$  is constant among nebulae, the  $C^{2+}/O$  ratio should follow an ionization curve in form similar to those produced by Kaler (1978*a*) for various ions of neon, argon, and chlorine. In these curves, the ionic abundance is plotted against  $\log T_*$  (central star temperature) for low-excitation nebulae, and  $Ex = He^{2+}/He$  for high-excitation objects. The ionization potentials for  $C^{2+}$  are very similar to the averages of those for  $He^+$ ,  $Cl^{2+}$  and  $Ar^{2+}$ ; Figure 1 shows their ionization curves. The dashed line indicates the mean of the curves for  $Ar^{2+}/O$  and  $Cl^{2+}/O$ , which are normalized at  $Ex = 0$  and then averaged. The dotted line shows  $He^+/He$ . For  $Ex > 0$ ,  $He^+/He$  is simply  $(1 - Ex)$ , and for  $Ex < 0$ , the curve is taken from Kaler's (1978*b*) empirical curve. Both curves are normalized at  $Ex = 0$ , and then averaged, which results in the solid line in Figure 1.

From the  $C^{2+}/H^+$  that result from equation (1) and Kaler's (1980)  $O/H$  ratios (or new ratios calculated from the most recent references in Table 1), we can calculate values of  $C^{2+}/O$ . The  $O/H$  ratios for nebulae that have  $He^{2+}/He^+ > 1$ , for which the correction for  $O^{3+}$  and  $O^{4+}$  becomes increasingly less reliable, and that were not considered in the above reference, are given in the footnotes to Table 1. In cases where the nebular excitation is high enough to preclude a calculation of  $O/H$  or is unknown, it is set equal to  $4 \times 10^{-4}$  (see these same footnotes). The resulting  $\log(C^{2+}/O)$  values from all references are also plotted in Figure 1. The ionization

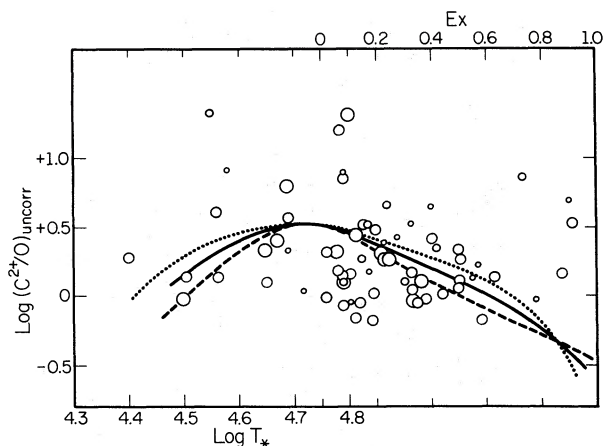


FIG. 1.—Uncorrected  $C^{2+}/O$  plotted against  $\log T_*$  and  $Ex = He^{2+}/He$ . All calculations from both columns (3) and (4) of Table 1 are included. The symbol sizes correspond to the weights assigned to the line intensities. The curves represent the expected ionization curves computed from ions of similar ionization potential—dashed line: mean curve for  $Ar^{2+}/O$ ,  $Cl^{2+}/O$ ; dotted line: curve from  $He^+/He$ ; solid line: mean of the two. The fit to the observed points is arbitrary.

curves were arbitrarily normalized by eye to pass through the points.

If there were no observational errors (which clearly must cause some of the scatter in Fig. 1), and if  $C/O$  were constant among nebulae,  $\log(C^{2+}/O)$  should follow the curve. If a point were to lie above the line, it would then indicate an overabundance of carbon for that object relative to the mean. The key for deriving carbon abundances here is that the *relative*  $C/O$  ratio can be found from the factor by which the point representing a nebula deviates from the arbitrarily scaled ionization curve. Thus

$$\log(C/O)(\text{preliminary}) = \log(C^{2+}/O)(\text{eq. 1}) - \log(C^{2+}/O)(\text{ionization curve}). \quad (2)$$

If the intensity of  $\lambda 4267$  was found both by scanner methods and by a method that required the correction procedure, the individual  $C/O$  were averaged if the weight assigned to the latter was 3 or 4; otherwise the former alone was used. These preliminary  $C/O$  were then scaled to the ultraviolet results (see § IIe below) to produce the first set of carbon-to-oxygen ratios, called  $(C/O)_1$ . Column (8) of Table 1 presents values of  $(C/O)_1$  for individual nebulae.

d) *Correction for Electron Density*

Figure 2 shows the above  $(C/O)_1$  plotted against  $\log x$ , where  $x = 10^{-2} N_e / (T_e)^{1/2}$ . The  $(C/O)_1$  correlate negatively with  $x$ , or  $N_e$ . The effect may be a secondary correlation involving real changes in  $C/O$ , or it may be the result of a systematic error in calculation. In the first instance, perhaps the set of large, low-surface-brightness nebulae, which have low densities, are overabundant in carbon. These objects have central stars in the lower-left (high temperature-low luminosity) portion of the (log

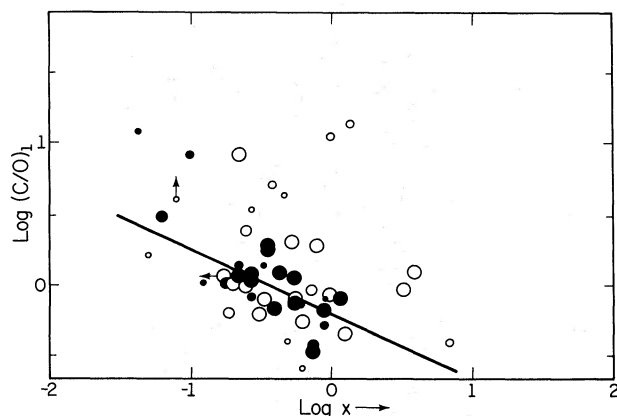


FIG. 2.—Relative log C/O as computed from the ionization curve of Fig. 1 and scaled to the UV data,  $(C/O)_1$ , plotted against  $\log x$  (from [O II] where possible), where  $x = 10^{-2} N_e/T_e)^{1/2}$ . The line intensities of Table 1 have been averaged (see text); symbol sizes correspond to the assigned weights. Nebulae for which the density can be computed from the  $\lambda 4267$  reference are represented by shaded symbols. The line shows the least-squares fit for the shaded symbols of weights 3 and 4 where the error is assumed to be shared by both variables.

$L - \log T$ -plane, and such a result is suggested by Renzini (1979). It seems much more likely, however, that the effect in Figure 2 reflects systematic error caused by the differential effect between the ionization balance of  $C^{2+}$  and the ions that are used in the construction of the ionization curve in Figure 1. This curve is an average, appropriate to the mean density of all nebulae considered. If the density is high, the ionization level of the nebula is suppressed as recombinations occur at a higher rate. For high density,  $Ex$  is too small relative to the standard curve, and the nebula is placed too far to the left in Figure 1. This effect will be important in the abundance calculations at higher excitation. The  $C^{2+}/C$  ratio is also dependent on  $N_e$ , but in a complicated way that depends on the amount of carbon in each ionization state. These phenomena certainly contribute to the scatter in Figure 2. The exact correction for this effect would require detailed modeling, which is inconsistent with the empirical approach that is developed herein. However, note that without eventual modeling, it cannot be known whether some residual effect involving real abundance variations is present.

Since a density dependence is expected, it is assumed here that its effect produces all the variation seen in Figure 2. We may then correct empirically by fitting a least-squares regression line through the data points. We ought to fit a family of lines as a function of excitation, but there are insufficient data for this procedure, and all the nebulae are treated together. A fit to the best determined points of Figure 2, in which the two axes share the error equally, yields

$$\log (\overline{C/O})_1 = -0.222 - 0.469 \log x . \quad (3)$$

Only points with weights 3 and 4 were used, and for which the electron density is known from one of the references from which the  $\lambda 4267$  intensity was taken (shaded in Fig. 2).

An excess of C/O with regard to the mean will again be displayed by a point above the regression line. We can now derive a corrected relative C/O,

$$\log (C/O)_{\text{rel}} = \log (C/O)_1 (\text{from eq. [2]}) \\ - \log (\overline{C/O})_1 (\text{mean line eq. [3]}) . \quad (4)$$

#### e) Absolute Scaling to Ultraviolet Data

All that is left now is to find the appropriate scaling factor for the relative C/O ratios derived from equation (4). Several of the nebulae in Table 1 have had C/H ratios derived from the far-ultraviolet lines. Footnote *b* in column (1) of Table 1 and a reference in column (12) indicate the eight nebulae used for the scaling. The *IUE* results are given double weight, and NGC 7027, NGC 7662, and IC 418, which are the best observed sources, are given triple weight. The mean error of the scaling factor is  $\pm 25\%$ .

Columns (9) and (10) in Table 1 present the final results for both C/O and C/H, called  $(C/O)_2$  and  $(C/H)_2$ . An estimate of the relative merit of these abundances is given in column (11), again as a weight scale from 1 to 4. These are taken from the weight for  $I(\lambda 4267)$  (col. [7]), which is reduced by one if the electron density was taken from a source other than that in column (5), and may be further subjectively reduced if any of the various input parameters do not seem to be well known. The  $(C/O)_2$  are the best currently attainable values; they should be superior to the  $(C/O)_1$ , which do not contain the density correction.

### III. DISCUSSION AND CONCLUSIONS

#### a) Analysis of the Data

The data are analyzed graphically in Figures 3, 4, and 5, and quantitatively in Table 2. We can use the data to best advantage in evaluating relative carbon enrichments

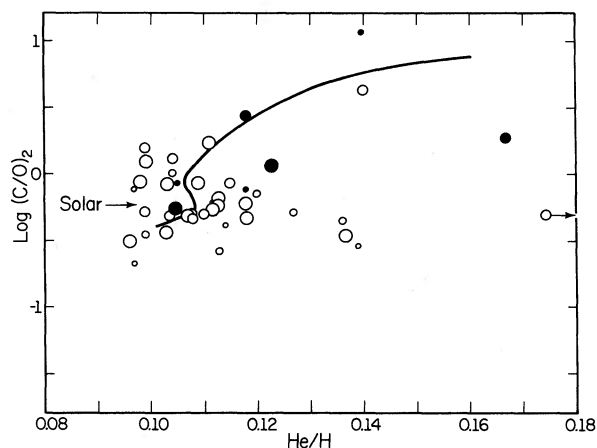


FIG. 3.—Final  $\log (C/O)_2$ , after correction for the electron density correlation of Fig. 2 and scaling to the ultraviolet data, plotted against He/H. Symbol sizes correspond to assigned weights; shaded symbols represent nebulae for which  $Ex = He^{2+}/He > 0.5$ . The curve is the theoretical correlation after third dredge-up taken from Becker and Iben (1980). The indicated solar value is from Lambert (1978).

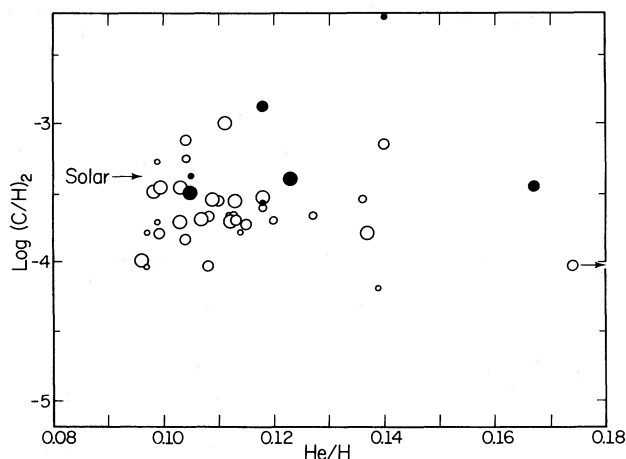


FIG. 4.—Final  $\log(C/H)_2$  plotted against  $He/H$ . See the caption to Fig. 3 for explanation of symbols.

among nebulae, and in particular in testing BI's theoretical contention that the envelopes of stars that form planetaries are often heavily enriched in carbon by nuclear processes, and that  $C/O$  should be a strong function of  $He/H$ .

Figure 3 shows  $\log(C/O)_2$  from Table 1 plotted against  $He/H$ , where the latter are taken from Kaler (1978b, 1980). The solid line shows BI's curve taken from their Figure 10 for conditions after the third dredge-up. It is evident from Figure 3 that the points do not fit the curve and do not support the theoretical prediction. It must be emphasized here that *only the relative C/O ratios have real merit*. The absolute values depend on the scaling to the UV results, and consequently on the selection of values to be used, current problems in the modeling of nebulae that are needed to interpret the UV data, and so forth. Consequently the formal  $\pm 25\%$  scaling error does not reflect the true error, which cannot be known at this time.

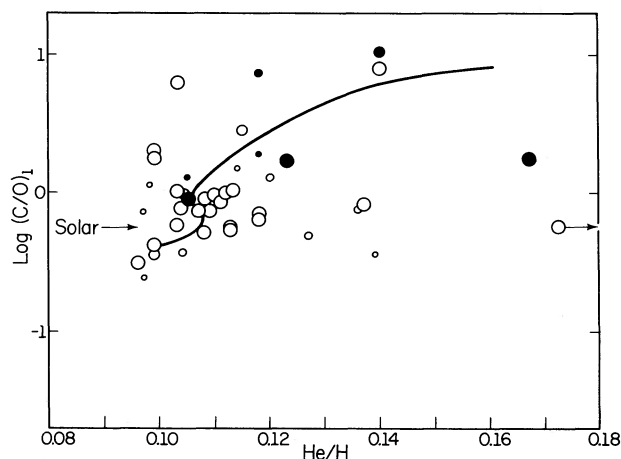


FIG. 5.— $\log(C/O)_1$ , the values before correction for electron density, scaled to the ultraviolet data, and plotted against  $He/H$ . See the caption to Fig. 3 for explanation of symbols.

TABLE 2  
MEAN AND MEDIAN  $C/O$  AND  $C/H^a$

A. ABUNDANCE GROUPS				
He/H (1)	$\overline{(C/O)}_2$ (2)	$10^4(C/H)_2$ (3)	$(C/O)_1$ (4)	No. (5)
$\leq 0.105$ .....	$0.76 \pm 0.09$ 0.78	$3.1 \pm 0.6$ 3.3	$0.89 \pm 0.16$ 0.83	13
$> 0.105$ .....	$0.66 \pm 0.07$	$2.8 \pm 0.5$	$0.93 \pm 0.14$	16
$\leq 0.120$ .....	0.56	2.1	0.83	
$> 0.120^b$ .....	$1.23 \pm 0.63$ 0.47	$2.8 \pm 1.0$ 1.9	$2.4 \pm 1.2$ 0.69	6
B. AGE GROUPS				
Age Group <sup>c</sup> (6)	$\overline{(C/O)}_2$ (7)	$10^4(C/H)_2$ (8)	$(C/O)_1$ (9)	No. (10)
1 .....	0.84 0.84	1.9 1.9	2.9 2.9	1
2 <sup>d</sup> .....	$1.04 \pm 0.37$ 0.57	$2.8 \pm 0.6$ 1.9	$1.9 \pm 0.7$ 0.75	10
3 .....	$0.81 \pm 0.37$ 0.52	$3.0 \pm 1.2$ 2.0	$0.95 \pm 0.53$ 0.43	3
4 .....	$0.71 \pm 0.08$ 0.61	$3.0 \pm 0.5$ 2.6	$0.82 \pm 0.08$ 0.81	12
5 .....	$0.64 \pm 0.16$ 0.43	$3.6 \pm 1.0$ 2.0	$0.77 \pm 0.12$ 0.81	8

<sup>a</sup> For each data set, the upper number gives the mean (with mean error) and the lower the median.  $\overline{(C/O)}_1$  gives mean  $C/O$  before correction for  $N_e$ , scaled to the UV.  $\overline{(C/O)}_2$ ,  $(C/H)_2$  are scaled means including the  $N_e$  correction.  $No.$  is the number of nebulae in each group.

<sup>b</sup> If NGC 6778 is dropped, columns (2), (3), and (4) read  $0.42 \pm 0.05$ ,  $1.67 \pm 0.39$ ,  $0.66 \pm 0.15$ , respectively.

<sup>c</sup> See Kaler 1980.

<sup>d</sup> If NGC 6778 is dropped, columns (7), (8), and (9) read  $0.65 \pm 0.11$ ,  $2.1 \pm 0.4$ ,  $0.93 \pm 0.16$ .

It is quite likely that the absolute scaling will slide up or down with new UV data and better interpretation. But the relative results presented here should not be so affected. Figures 4 and 5 show  $(C/H)_2$  and  $(C/O)_1$  plotted against  $He/H$ . All three figures (Figs. 3–5) have similar appearances.

Tables 2 and 3 present the results of a quantitative analysis of the data. In Table 2A, Figures 3, 4, and 5 are divided into three helium groups as shown in column (1). Columns (2), (3), and (4) then show the weighted mean (upper number) and the median (lower number)  $(C/O)_2$ ,  $(C/H)_2$ , and  $(C/O)_1$  for each group. High excitation nebulae ( $E_x > 0.5$ ), for which  $O/H$  (and similarly  $C/H$  and  $C/O$ ) is likely to be uncertain, are excluded (note the position of high-excitation points in Fig. 1). These high-excitation nebulae are shown as shaded symbols in Figures 3, 4, and 5 and will be discussed below. Low-excitation objects ( $\log T_* < 4.65$ ) are automatically excluded, as  $He/H$  is not known for them because of significant neutral helium. The fourth column gives the number of nebulae in each group. The error is the mean error of the mean.

TABLE 3  
MEAN AND MEDIAN C/O AND C/H FOR THE THREE  
EXCITATION GROUPS AND SOLAR VALUES<sup>a</sup>

	$(C/O)_2$	$10^4 (C/H)_2$	No.
Low Excitation .....	$3.1 \pm 2.4$ 2.7	$10.4 \pm 5.3$ 8.3	6
Middle Excitation .....	$0.78 \pm 0.12$ 0.52	$2.9 \pm 0.4$ 2.1	35
High Excitation <sup>b</sup> .....	$2.0 \pm 1.3$ 1.5	$8.7 \pm 6.7$ 4.4	7
Solar .....	0.56	4.7	

<sup>a</sup> For each data set, the upper number gives the mean (with mean error) and the lower the median.  $(C/O)_1$  gives mean C/O before correction for  $N_e$ , scaled to the UV.  $(C/O)_2$ ,  $(C/H)_2$  are scaled means including the  $N_e$  correction. No. is the number of nebulae in each group.

<sup>b</sup> If NGC 7008 is dropped,  $(C/O)_2$  and  $(C/H)_2$  are  $1.5 \pm 0.4$  and  $5.8 \pm 1.7 \times 10^{-4}$ .

There are no significant differences among the three groups. The high He/H group has a high C/O because of the one high point (NGC 6778) at He/H = 0.14, but the error is concomitantly high because of it. Averages excluding this object are given in footnote b of the table. The medians, which are perhaps more significant, and the means without NGC 6778, show a downward trend for C/O as He/H increases rather than the predicted upward one.

Table 2B (columns [6] through [10]) given an analogous set of data wherein the nebulae are divided according to Kaler's (1980) age group (groups 1 through 5 progress from the extreme halo to the extreme disk). Footnote d shows the mean for group 2 with NGC 6778 again excluded. The means and medians for C/O and C/H exhibit no significant or consistent trends. We might expect that one or the other should show a galactic variation similar to that found for O/H. If one is present, it is lost in the rather large scatter of points.

The mean and the median  $(C/O)_2$  and  $(C/H)_2$  for the three excitation groups are given separately in Table 3, together with solar values from Lambert (1978). Although the nebulae of middle excitation, which are the most reliable, agree well with the solar value, caution is advised because of uncertainties in the calibration and because of effects discussed below.

#### b) Problems in Analysis and Interpretation

From Table 3, we see that the C/O and C/H ratios for both the high ( $Ex > 0.5$ ) and low ( $\log T_* < 4.65$ ) excitation sets are high. The means for the high-excitation set are overweighted by one very high point, NGC 7008; the resulting lower values are given in footnote b to Table 3. The mean values for  $(C/O)_1$  show a closely similar trend. The effect can also be seen in Figure 1; the middle excitation objects scatter around the curve, whereas the other two sets tend to lie above it. The ionization curve falls from both sides of center, but the distribution of points tends toward flatness. Taken at face value, it would seem that the high and low excitation nebulae might

suffer carbon enrichment. The high-excitation set, indicated by filled symbols in Figures 3 and 4, in fact shows more of a qualitative agreement with the BI curve. But there are other effects which must be considered. First, the ionization curve might not be applicable to  $C^{2+}$  for extreme excitation levels; for example, the  $Ar^{2+}$  and  $Cl^{2+}$  data upon which the curve is based are deficient below  $\log T_* = 4.65$ . But the helium, argon, and chlorine data generally agree reasonably well with one another and there is no compelling reason to believe that the curve is not at least approximately correct.

Second is the problem of fluorescence. The  $\lambda 4267$  line could be produced at low excitation by direct stellar excitation of  $C^+$  (see Seaton 1968; Kaler 1972). Grandi's (1976) calculations indicate that fluorescence is not a problem, at least at the excitation level of the Orion Nebula. There is no *a priori* or theoretical reason to believe that the low-excitation objects should be carbon rich. It seems more likely that the high values in Table 2 are the result of some flaw or lack in the analysis or in our physical understanding, but this remains to be proved. Clearly, ionization in this excitation regime needs to be studied in much more detail.

Third, and perhaps most important, are selection effects. We generally have data on  $\lambda 4267$  only when it is already strong. Nebulae with low C/H may well not be detected. This problem is particularly important for the high-excitation objects, where  $C^{2+}$  would be expected to have a low ionic abundance in the first place. For these we might observe  $\lambda 4267$  only when C/O is abnormally large. Selection may explain why the distribution of points in Figure 1 is relatively flat, and does not drop with the ionization curve for high Ex. It is not possible at this time, however, to evaluate quantitatively the effects of selection.

The nebulae used in the calibration of the optical data to the ultraviolet include objects of both high and low excitation. If these are excluded, the calibration factor increases by an insignificant 15%.

#### c) Conclusions

One reasonably definite conclusion can be drawn from this review of the data: the general trend of points does not fit the predicted theoretical relation between C/O and He/H. The similarity of the  $(C/O)_1$  and  $(C/O)_2$  analysis shows that this result is not influenced by the electron density effect described in § II d.

At first, this result would seem to argue against the theory, but consider that the abundances here refer to atomic carbon. Much of the carbon may be locked in molecular form or in grains. Note also that some few points of high excitation show something of a qualitative fit to the curve. We might speculate that in nebulae with high stellar temperatures, more carbon is in atomic form. However, there are insufficient data for any firm conclusions along this line; selection effects are particularly important and cannot be properly evaluated. As a test of this hypothesis, the deficiency of observed C/O against the theoretical prediction was compared to the ratio of infrared flux (from Cohen and Barlow 1974, 1980) to H $\beta$  flux; no correlations are seen. Other possible reasons for

the lack of fit are discussed in BI. They include such things as error in the cross section for capture of an  $\alpha$ -particle by  $^{12}\text{C}$ , and conversion of  $^{12}\text{C}$  into  $^{14}\text{N}$  in the stellar envelope.

The distribution of points, and the average ratios of the most reliable set of data, are similar to solar determinations. But any conclusions as to absolute C/O and C/H are critically dependent on the ultraviolet scaling, and should be viewed with caution. Only the relative results should be considered as reliable. Carbon enhancements as a function of the evolutionary state of the star (Renzini 1979) cannot be assessed until the electron density correlation of Figure 2 is quantitatively understood, and the effects of selection are minimized by further observation. Finally, the origin of the high ratios derived for both low- and high-excitation objects cannot be properly understood until the ionization balance is examined in more detail. At this point, we can say only that the present data do not support BI's theory, even though they may not deny its validity.

#### IV. SUMMARY

C/O and C/H ratios have been calculated from  $\lambda 4267$  C II for 53 planetary nebulae by comparison of  $\text{C}^{2+}/\text{O}$  with a mean ionization curve, including correction for density effects, and by calibration with ultraviolet data. In the process, a catalog of corrected line intensity data is presented, which will provide a data base for future refinements in the abundance calculations and for comparison against recombination theory and abundances provided from ultraviolet data.

The data are used to examine the prediction that carbon is enriched in planetaries by convective dredge-up in asymptotic giant-branch stars before ejection of the nebula. Becker and Iben (1980) calculate that C/O should

rise sharply with He/H during the third dredge-up phase, the thermal pulsing stage, of the star's evolution. The data do not generally support this theory. As He/H increases, the average C/O and C/H remain essentially unchanged, although there is a very wide scatter among individual nebulae. A small number of nebulae of mostly high excitation do fall qualitatively near the theoretical curve, but the data on objects of this sort are too sparse to enable us to draw any firm conclusions. The average C/O and C/H are near solar, but this result depends entirely on the calibration to the ultraviolet data and is subject to change as the latter improve. The conclusions of this paper more involve the relative C/O and C/H than they do the absolute values.

There are a variety of explanations for the general disagreement between theory and observation, which are discussed in Becker and Iben (1980). The theory may be wrong, and carbon dredge-up may not occur, or carbon may be destroyed along the way. Or, perhaps the carbon in planetaries is largely not in atomic form because of grain or molecule formation. The matter should be solvable with further ultraviolet observations.

For the future, special attention should be paid to high-excitation objects in order to minimize the effects of observational selection. Detailed modeling is also needed to examine nebular ionization, in order to assess the reality of the higher abundance ratios calculated for extreme high- and low-excitation objects, and to study the electron density correction that was used to obtain the final C/O ratios.

This work was supported by National Science Foundation grant AST 78-23647 to the University of Illinois. I would like to thank Drs. S. Becker, I. Iben, and J. Lutz for helpful discussion and commentary.

#### REFERENCES

- Aller, L. H., and Czyzak, S. J. 1970, *Ap. J.*, **160**, 929.  
 ———. 1979, *Ap. Space Sci.*, **62**, 397.  
 Aller, L. H., Czyzak, S. J., and Buerger, E. G. 1970, *Ap. J.*, **162**, 783.  
 Aller, L. H., Czyzak, S. J., and Kaler, J. B. 1968, *Ap. J.*, **151**, 187.  
 Aller, L. H., and Epps, H. W. 1975, *Ap. J.*, **197**, 175.  
 Aller, L. H., and Kaler, J. B. 1964a, *Ap. J.*, **139**, 1074.  
 ———. 1964b, *Ap. J.*, **140**, 621.  
 ———. 1964c, *Ap. J.*, **140**, 936.  
 Aller, L. H., Kaler, J. B., and Bowen, I. S. 1966, *Ap. J.*, **144**, 291.  
 Aller, L. H., Kaler, J. B., and Czyzak, S. J. 1976, *Ap. J.*, **203**, 636.  
 Aller, L. H., and Keyes, C. D. 1981, preprint.  
 Aller, L. H., Keyes, C. D., Czyzak, S. J., and Shields, G. A. 1981, preprint.  
 Aller, L. H., Keyes, C. D., Ross, J. E., and O'Mara, B. J. 1981, preprint.  
 Aller, L. H., Krupp, E., and Czyzak, S. J. 1969, *Ap. J.*, **158**, 953.  
 Aller, L. H., and Menzel, D. H. 1945, *Ap. J.*, **102**, 239.  
 Aller, L. H., Ross, J. E., O'Mara, B. J., and Keyes, C. D. 1981, preprint.  
 Aller, L. H., and Walker, M. F. 1965, *Ap. J.*, **141**, 1318.  
 Aller, L. H., and Wares, G. 1969, *Nature*, **221**, 646.  
 Becker, S. A., and Iben, I., Jr. 1980, *Ap. J.*, **237**, 111 (BI).  
 Bohlin, R. C., Harrington, J. P., and Stecher, T. P. 1978, *Ap. J.*, **219**, 575.  
 Bohlin, R. C., Marioni, P. A., and Stecher, T. P. 1975, *Ap. J.*, **202**, 415.  
 Brocklehurst, M. 1971, *M.N.R.A.S.*, **153**, 471.  
 Cohen, M., and Barlow, M. J. 1974, *Ap. J.*, **193**, 401.  
 ———. 1980, *Ap. J.*, **238**, 585.  
 Czyzak, S. J., and Aller, L. H. 1970, *Ap. J.*, **162**, 495.  
 ———. 1973, *Ap. J.*, **181**, 817.  
 ———. 1979, *M.N.R.A.S.*, **188**, 229.  
 Czyzak, S. J., Aller, L. H., and Kaler, J. B. 1968, *Ap. J.*, **154**, 543.  
 ———. 1971, *Ap. J.*, **168**, 405.  
 Czyzak, S. J., Aller, L. H., Kaler, J. B., and Faulkner, D. J. 1966, *Ap. J.*, **143**, 327.  
 Czyzak, S. J., Aller, L. H., and Leckrone, D. 1969, *Ap. J.*, **157**, 1225.  
 Grandi, S. A. 1976, *Ap. J.*, **206**, 658.  
 Harrington, J. P., Lutz, J. H., Seaton, M. J., and Stickland, D. J. 1980, *M.N.R.A.S.*, **191**, 13.  
 Harrington, J. P., Seaton, M. J., Lutz, J. H., and Adams, S. 1981, *M.N.R.A.S.*, in press.  
 Kaler, J. B. 1972, *Ap. J.*, **173**, 601.  
 ———. 1976, *Ap. J. Suppl.*, **31**, 517.  
 ———. 1978a, *Ap. J.*, **225**, 527.  
 ———. 1978b, *Ap. J.*, **226**, 947.  
 ———. 1979, *Ap. J.*, **228**, 163.  
 ———. 1980, *Ap. J.*, **239**, 78.  
 ———. 1981, *Ap. J.*, **243**, in press.  
 Kaler, J. B., Aller, L. H., Czyzak, S. J., and Epps, H. W. 1976, *Ap. J. Suppl.*, **31**, 163.  
 Kaler, J. B., Czyzak, S. J., and Aller, L. H. 1968, *Ap. J.*, **153**, 43.  
 Kondratyeva, L. N. 1978, *Astr. Zh.*, **55**, 334.  
 Lambert, D. L. 1978, *M.N.R.A.S.*, **182**, 249.  
 Lee, P., Aller, L. H., Kaler, J. B., and Czyzak, S. J. 1974, *Ap. J.*, **192**, 159.  
 Lutz, J. H. 1981, *Ap. J.*, in press.  
 Peimbert, M., and Costero, R. 1969, *Bol. Obs. Tonantzintia y Tacubaya*, **5**, 3.  
 Pengelly, R. M. 1963, Ph.D. thesis, University of London.

- Perek, L., and Kohoutek, L. 1967, *Catalogue of Galactic Planetary Nebulae* (Prague: Czechoslovakian Acad. of Sci.).
- Perinotto, M., Panagia, N., and Benvenuti, P. 1980, *Astr. Ap.*, **85**, 332.
- Pottasch, S. R., Wesselius, P. R., and van Duinen, R. J. 1978, *Astr. Ap.*, **70**, 629 (PWD).
- Renzini, A. 1979, in *IAU 4th European Regional Meeting in Astr.: Stars and Stellar Systems*, ed. B. E. Westerlund (Dordrecht: Reidel), p. 155.
- Seaton, M. J. 1968, *M.N.R.A.S.*, **139**, 129.
- Torres-Peimbert, S., and Peimbert, M. 1977, *Rev. Mexicana Astr. Ap.*, **2**, 181 (TPP).
- . 1979, *Rev. Mexicana Astr. Ap.*, **4**, 341.
- Torres-Peimbert, S., Peimbert, M., and Daltabuit, E. 1980, *Ap. J.*, **238**, 133.

JAMES B. KALER: Department of Astronomy, 341 Astronomy Building, University of Illinois, Urbana, IL 61810